



# Altered intra- and inter-hemispheric functional dysconnectivity in schizophrenia

Yuan Zhang<sup>1,2</sup> · Zhongxiang Dai<sup>3</sup> · Yu Chen<sup>4</sup> · Kang Sim<sup>5,6</sup> · Yu Sun<sup>1</sup> · Rongjun Yu<sup>7,8</sup>

Published online: 9 August 2018  
© Springer Science+Business Media, LLC, part of Springer Nature 2018

## Abstract

Despite convergent evidence suggesting that schizophrenia is a disorder of brain dysconnectivity, it remains unclear whether intra- or inter-hemispheric deficits or their combination underlie the dysconnection. This study examined the source of the functional dysconnection in schizophrenia. Resting-state fMRI was performed in 66 patients with schizophrenia and 73 matched healthy controls. Functional brain networks were constructed for each participant and further partitioned into intra- and inter-hemispheric connections. We examined how schizophrenia altered the intra-hemispheric topological properties and the inter-hemispheric nodal strength. Although several subcortical and cingulate regions exhibited hemispheric-independent aberrations of regional efficiency, the optimal small-world properties in the hemispheric networks and their lateralization were preserved in patients. A significant deficit in the inter-hemispheric connectivity was revealed in most of the hub regions, leading to an inter-hemispheric hypo-connectivity pattern in patients. These abnormal intra- and inter-hemispheric network organizations were associated with the clinical features of schizophrenia. The patients in the present study received different medications. These findings provide new insights into the nature of dysconnectivity in schizophrenia, highlighting the dissociable processes between the preserved intra-hemispheric network topology and altered inter-hemispheric functional connectivity.

**Keywords** Schizophrenia · Hemispheric asymmetry · Inter-hemispheric connectivity · Resting-state functional connectivity · Graph theory

## Introduction

Schizophrenia, a severe neuropsychiatric disorder characterized by cognitive and affective deficits (Howes and Murray 2014), has been found to be associated with aberrant hemispheric specialization of cognitive functions (Collinson et al. 2009). In particular, impaired speech processing related to a leftward morphological abnormality in the temporal lobe

(Shenton et al. 2001) has been proposed as a key cognitive factor in the manifestation of the symptoms of schizophrenia (Mesholam-Gately et al. 2009). Moreover, heterogeneity in the clinical features of schizophrenia suggests that the neural mechanisms of these features change on both a local and global scale due to the illness (Friston et al. 2016). In fact, a recent conceptualization proposes that the human brain forms a large-scale network of interconnected regions within the

✉ Yu Sun  
yusun@zju.edu.cn

✉ Rongjun Yu  
psyjr@nus.edu.sg

<sup>1</sup> Key Laboratory for Biomedical Engineering of the Ministry of Education, Department of Biomedical Engineering, Zhejiang University, Zhejiang 310000, China

<sup>2</sup> Department of Psychiatry and Behavioral Sciences, Stanford University, Stanford, CA, USA

<sup>3</sup> Department of Computer Science, National University of Singapore, Singapore, Singapore

<sup>4</sup> School of Computer Engineering, Nanyang Technological University, Singapore, Singapore

<sup>5</sup> Department of General Psychiatry, Institute of Mental Health, Singapore, Singapore

<sup>6</sup> Department of Research, Institute of Mental Health, Singapore, Singapore

<sup>7</sup> Department of Psychology, National University of Singapore, Block AS4, #02-07, 9 Arts Link, Singapore 117570, Singapore

<sup>8</sup> Graduate School for Integrative Sciences and Engineering, National University of Singapore, Singapore, Singapore

human connectome (Sporns 2011). Dysconnection among brain regions may represent a derailment of cognitive functions in schizophrenia (Fornito et al. 2012; Friston et al. 2016; Pettersson-Yeo et al. 2011). For instance, rightward reductions were revealed in the anterior-posterior frontal connectivity (Shapleske et al. 2002), while leftward reductions were reported in a temporal network interconnecting the frontal lobe, insula, and temporo-occipital lobes (Ellison-Wright and Bullmore 2009). In addition, accumulating evidence suggests that patients with schizophrenia suffer from impaired inter-hemispheric interactions that are associated with symptom severity (S. Guo et al. 2013; W. Guo et al. 2014; Hoptman et al. 2012). However, it remains unclear whether intra- or inter-hemispheric deficits or the combination of both underlie the dysconnection in schizophrenia.

Graph theoretical analysis, which enables quantitative assessment of topological properties of the brain network (Bullmore and Sporns 2009; He and Evans 2010), has been utilized to investigate the topological alterations of functional brain networks in schizophrenia (Fornito et al. 2012; He and Evans 2010; Y. Liu et al. 2008; van den Heuvel and Fornito 2014). Specifically, a substantial number of studies have reported abnormal network architectures, including a decreased clustering coefficient and local efficiency (Fornito et al. 2012; Y. Liu et al. 2008), altered global efficiency (Alexander-Bloch et al. 2010; Y. Liu et al. 2008; Lynall et al. 2010), decreased modularity (Alexander-Bloch et al. 2010; Sun et al. 2017b; Q. Yu et al. 2011), and disrupted rich club organization (highly connected hub regions) (van den Heuvel et al. 2013; Q. Yu et al. 2013), suggesting a subtle seemingly random network topology in schizophrenia (Rubinov et al. 2009). These abnormal network topologies also relate to clinical symptoms (van den Heuvel and Fornito 2014). Of note, these alterations in functional networks were identified exclusively at a “whole-brain” level.

Only until recently, there have been a few studies beginning to examine the topological organization at the hemispheric level in brain functional networks (Gotts et al. 2013; Tian et al. 2011). For instance, Tian and colleagues revealed that the hemispheric networks exhibited small-world properties (high local clustering with short paths between brain regions) that were compatible with those at the whole-brain level in healthy adults, suggesting that the efficiency of information processing within each hemisphere could be similar to that in the whole brain (Tian et al. 2011). Gotts et al. (2013) further reported two distinct forms of functional lateralization in the human brain. In the left hemisphere, there is a preference for intra-hemispheric interactions, whereas in the right hemisphere there is an integration of interactions between both hemispheres. In our recent study, we examined schizophrenia-related alterations in hemispheric structural networks and found a reduced hemispheric asymmetry in patients (Sun et al. 2017a), providing some of the first quantitative evidence of lateralized hemispheric dysconnectivity. While it

is commonly assumed that functional connectivity reflects underlying structural brain connectivity, the nature of the structure-function relationship remains unclear (Damoiseaux and Greicius 2009; Z. Wang et al. 2015) and observations concerning one modality cannot be directly applied to the other (Honey et al. 2009). In fact, recent studies have reported a complex relationship between structural and functional connectivity in patients with schizophrenia (Skudlarski et al. 2010; Sun et al. 2017b).

In this study, we examined the source of the functional dysconnection (i.e., intra- or inter-hemispheric or both) in schizophrenia by combining resting-state fMRI and graph theoretical analysis. Specifically, we first assessed intra-hemispheric alterations in terms of the hemispheric functional network topology, including the small-world properties, global and local network efficiencies, and nodal characteristics. Although aberrant lateralization has been linked to schizophrenia (Artiges et al. 2000; Bleich-Cohen et al. 2009; Razafimandimby et al. 2007; Sommer et al. 2001), it remains unclear how altered focal laterality might affect brain network asymmetry. Thus, we further examined alterations in network asymmetry based on the hemispheric network metrics. We hypothesized that intra-hemispheric alterations occur in both global and regional topological properties in schizophrenia, which further affect the network asymmetry. In addition, recent studies reported abnormalities in connectivity between a region and its contralateral counterpart in schizophrenia (S. Guo et al. 2013; W. Guo et al. 2014; Hoptman et al. 2012), but it remains unclear whether abnormalities exist only in pairwise interactions between two regions or in regional connectivity with the whole contralateral hemisphere. Thus, we examined schizophrenia-related inter-hemispheric alterations in terms of nodal strength connecting the contralateral hemisphere. We hypothesized that schizophrenia is related to inter-hemispheric hypo-connectivity. We further hypothesized that intra- and inter-hemispheric alterations are correlated with the clinical features of schizophrenia.

## Methods and materials

### Subjects

The data used in this study were from the Center for Biomedical Research Excellence (COBRE), University of New Mexico, including 72 patients with schizophrenia and 76 healthy controls of comparable age. One patient was excluded due to the presence of DSM-IV Axis I diagnoses of other disorders and two dropouts were excluded from the healthy controls. Participants from the healthy group were free of mental disorders, neurological diseases, history of substance dependence and clinically significant head trauma. The patients' psychopathology and symptom severity were

assessed by the positive and negative syndrome scale (PANSS) (Kay et al. 1987). The study was approved by the National University of Singapore Institutional Review Board.

## Data acquisition

Structural and functional MRI scans were acquired from each subject in a single session with a 3-T Siemens Trio scanner. Foam padding/paper tapes were used to reduce head motion. All images were acquired parallel to anterior-posterior commissures with an auto-align technique. A whole-brain high-resolution T1-weighted MR image was obtained in a coronal view using a five-echo magnetization-prepared rapid gradient-echo sequence (MP-RAGE) with the following parameters: repetition time (TR) = 2.53 s, echo times (TE) = [1.64, 3.50, 5.36, 7.22, 9.08] ms, flip angle = 7°, slice thickness = 1 mm, field of view (FOV) = 256 × 256 mm<sup>2</sup>, resolution = 256 × 256. A total of 150 volumes of single-shot full k-space echo-planar imaging (EPI) was obtained with ramp sampling correction using the intercommissural line (AC-PC) as a reference, using the following parameters: TR = 2000 ms, TE = 29 ms, FOV = 256 × 256 mm<sup>2</sup>, matrix = 64 × 64, slice number = 33, voxel size = 3 × 3 × 4 mm<sup>3</sup> (refer to <http://coins.mm.org/dx> for more details).

## Data preprocessing and network construction

Data preprocessing and brain network construction have been described previously in detail (Sun et al. 2017a, b, c; Sun et al. 2014). Briefly, the first 5 volumes were removed due to signal equilibration effects. The remaining images were corrected for slice timing, realigned to the first volume (the original 6th volume) to correct for head motion, and coregistered to each structural T1 image. Each structural T1 image was segmented into cerebrospinal fluid (CSF) tissue, grey matter, and white matter maps. Nuisance signal correction was then performed based on the 24 head motion parameters, the global signal, white matter, and CSF signals. The resulting functional images were normalized into a standard stereotaxic space (Montreal Neurologic Institute), resampled to 3 × 3 × 3 mm<sup>3</sup>, and spatially smoothed with a 6-mm full-width half maximum (FWHM) Gaussian kernel. The obtained image time series were band-pass filtered (0.01–0.08 Hz) to remove low-frequency noises such as scanner drifts and high-frequency interferences including cardiac and respiratory activities (Fox and Raichle 2007). For more details about the data preprocessing, please refer to Yan and Zang (2010) (Yan and Zang 2010).

To reduce the impact of excessive head motion on resting-state functional connectivity (Power et al. 2012; Van Dijk et al. 2012), we excluded participants with head movements larger than 3 mm of translation or 3 degrees of rotation in any direction. As a result, one participant was excluded from the control

group, leaving 73 healthy controls (male/female: 50/23) for data analysis. Moreover, the Jenkinson frame-wise displacement (FD) was calculated to account for group-level residual effects of head motion (Jenkinson et al. 2002). Participants with mean FD that was two standard deviation (SD) above the group-averaged FD were discarded from the subsequent analysis (Yan et al. 2013). As a result, five patients were further excluded, leaving 66 patients (male/female: 53/13) for data analysis. Group difference on head motion was not significant. Demographic and clinical characteristics of the included participants are shown in Table 1.

Next, we parcellated the whole brain into 90 regions of interest (ROIs) based on the automated anatomical labelling (AAL) template (Tzourio-Mazoyer et al. 2002) (Table 2). Time series were averaged across voxels within each ROI. Pearson correlation was calculated for each pair of ROIs and used as a measure of functional connectivity strength (Zalesky et al. 2012). Fisher's Z-transformation was further applied to the correlation matrices to improve the distribution of functional connectivity (Yan et al. 2013). As such, each functional network was represented by a symmetric matrix (90 × 90), which was further separated into two hemispheric networks (45 × 45) and inter-hemispheric connections. Negative connectivity was further removed due to the ongoing debate about its physiological meanings (Anderson et al. 2011). A flow chart of the data analysis approach is shown in Fig. 1.

## Graph theoretical analysis of hemispheric brain network

Graph theoretical analysis has attracted significant attention in brain network research because it provides a powerful quantitative way to describe the segregation and integration of brain networks from the perspective of topological architecture (Bullmore and Sporns 2009; Watts and Strogatz 1998). Here, we conducted graph theoretical analysis using Brain Connectivity Toolbox (Rubinov and Sporns 2010). Prior to the analysis, each of the obtained hemispheric networks was thresholded at a sparsity value and then binarized. For a given network  $G$  with  $N$  nodes ( $N = 45$  in this work), sparsity ( $s$ ) is defined as the ratio of the actual edge number to the maximum possible number of edges in a network. The thresholding ensured that the wiring cost (the number of edges) of the network was the same in both groups. To avoid the impact of an arbitrary threshold on network properties, we adopted a wide range of sparsity (i.e., 10% ≤  $s$  ≤ 40%, with an interval of 1%).

At each sparsity, hemispheric network topology was assessed at both global and regional levels. Five network metrics, including three small-world measurements (i.e., clustering coefficient ( $C$ ), characteristic path length ( $L$ ), and small-worldness ( $\sigma$ )) and two efficiency measurements (i.e., global efficiency ( $E_{global}$ ), and local efficiency ( $E_{local}$ )) were adopted to examine schizophrenia-related alterations in global

**Table 1** Demographic and clinical characteristics of the subsamples<sup>a</sup>

Characteristic	Group (patients/controls = 66/73)		Statistics <i>p</i> -value
	Patients with Schizophrenia	Healthy Controls	
Age (years)	18–65 (38.2 ± 14.1)	18–65 (35.9 ± 11.6)	0.303 <sup>b</sup>
Education (years)	10–20 (13.1 ± 1.7) <sup>d</sup>	10–18 (13.9 ± 1.7) <sup>e</sup>	0.006 <sup>b</sup>
Male/Female	53/13	50/23	0.112 <sup>c</sup>
Handedness (R/L/A)	55/9/2	70/1/2	0.020 <sup>c</sup>
WAIS-Verbal	63–132 (98.2 ± 16.4) <sup>d</sup>	75–126 (106.7 ± 11.2) <sup>e</sup>	< 0.001 <sup>b</sup>
WAIS-Performance	61–129 (102.5 ± 16.9) <sup>d</sup>	76–139 (114.0 ± 12.3) <sup>e</sup>	< 0.001 <sup>b</sup>
WAIS-Sum	65–134 (99.8 ± 16.9) <sup>d</sup>	83–133 (111.7 ± 11.8) <sup>e</sup>	< 0.001 <sup>b</sup>
Age of onset (years)	5–61 (22.1 ± 8.8) <sup>f</sup>	–	–
Duration of illness (years)	0–47 (15.9 ± 12.4) <sup>f</sup>	–	–
Medication dose (mg/day)	0–1800 (357.5 ± 307.4) <sup>g</sup>	–	–
PANSS-positive symptoms	7–28 (14.9 ± 4.8)	–	–
PANSS-negative symptoms	8–29 (14.6 ± 4.8)	–	–
PANSS-general symptoms	16–56 (29.2 ± 8.6)	–	–
PANSS-total	35–94 (58.6 ± 14.2)	–	–

<sup>a</sup> Data are expressed as minimum – maximum (mean ± S.D.)

<sup>b</sup> The *p*-value was obtained using a two-sample two-tailed *t*-test

<sup>c</sup> The *p*-value was obtained using a two-tailed Pearson  $\chi^2$  test

<sup>d</sup> Data were missing for four patients with schizophrenia

<sup>e</sup> Data were missing for six healthy controls

<sup>f</sup> Data were missing for one patient with schizophrenia

<sup>g</sup> Data were missing for two patients with schizophrenia

Handedness, *R* right, *L* left, *A* ambidextrous; *WAIS* wechsler adult intelligence scale, *PANSS* positive and negative syndrome scale

topology of the hemispheric networks. For a given network  $G$  with  $N$  nodes, the clustering coefficient  $C$  is defined (Watts and Strogatz 1998) as:

$$C = \frac{1}{N} \sum_{i \in N} \frac{2E_i}{k_i(k_i - 1)} \quad (1)$$

where  $k_i$  is the number of edges connected to node  $i$ , and  $E_i$  is the number of triangles around the node (Rubinov and Sporns 2010). It measures the extent of the local density or cliquishness of a network.

The characteristic path length,  $L$ , of a network is defined as:

$$L = \frac{1}{N} \sum_{i \in N} \frac{\sum_{j \in N, j \neq i} \min\{L_{ij}\}}{N-1} \quad (2)$$

where  $\min\{L_{ij}\}$  is the shortest path length between node  $i$  and  $j$ . It measures the overall routing efficiency of the network.

The normalized clustering coefficient  $\gamma = C/C^{rand}$  and normalized characteristic path length  $\lambda = L/L^{rand}$  were further computed to facilitate the calculation of small-worldness ( $\sigma$ ) (Watts and Strogatz 1998). Here,  $C^{rand}$  and  $L^{rand}$  denote the average clustering coefficient and the average characteristic path length derived from an ensemble of 100 surrogate

random networks, which were generated by preserving the same number of nodes, edges, degree distribution and connectedness (Maslov and Sneppen 2002). Small-worldness is a unified metric that quantifies the balance between local segregation and global integration in a network. A network is considered small-world if it meets the following criteria:  $\sigma > 1$  ( $\sigma = \gamma/\lambda$ ) (Humphries et al. 2006).

To further assess the small-world properties of the networks in terms of information flow, global efficiency ( $E_{global}$ ) and local efficiency ( $E_{local}$ ) were calculated (Latora and Marchiori 2001).  $E_{global}$  is defined as the inverse of the harmonic mean of the shortest path length between each pair of regions (Achard and Bullmore 2007; Latora and Marchiori 2001):

$$E_{global} = \frac{1}{N(N-1)} \sum_{i \neq j \in N} \frac{1}{\min\{L_{ij}\}} \quad (3)$$

It quantifies the global efficiency of parallel information transfer in the network  $G$ .  $E_{local}$  is calculated by averaging global efficiency  $E_{global}(i)$  across all nodes:

$$E_{local} = \frac{1}{N} \sum_{i \in N} E_{global}(i) \quad (4)$$

**Table 2** Names and corresponding abbreviations of the regions of interest (ROIs)

Region name	Abbrev.	Class	Region name	Abbrev.	Class
Precentral gyrus	PreCG	Primary	Lingual gyrus	LING	Association
Superior frontal gyrus (dorsal)	SFGdor	Association	Superior occipital gyrus	SOG	Association
Orbitofrontal cortex (superior)	ORBsup	Paralimbic	Middle occipital gyrus	MOG	Association
Middle frontal gyrus	MFG	Association	Inferior occipital gyrus	IOG	Association
Orbitofrontal gyrus (middle)	ORBmid	Paralimbic	Fusiform gyrus	FFG	Association
Inferior frontal gyrus (opercular)	IFGoperc	Association	Postcentral gyrus	PoCG	Primary
Inferior frontal gyrus (triangular)	IFGtriang	Association	Superior parietal gyrus	SPG	Association
Orbitofrontal gyrus (inferior)	ORBinf	Paralimbic	Inferior parietal lobe	IPL	Association
Rolandic operculum	ROL	Association	Supramarginal gyrus	SMG	Association
Supplementary motor area	SMA	Association	Angular gyrus	ANG	Association
Olfactory	OLF	Paralimbic	Precuneus	PCUN	Association
Superior frontal gyrus (medial)	SFGmed	Association	Paracentral lobule	PCL	Association
Orbitofrontal gyrus (medial)	ORBmed	Paralimbic	Caudate nucleus	CAU	Subcortical
Gyrus rectus	REC	Paralimbic	Putamen	PUT	Subcortical
Insula	INS	Paralimbic	Pallidum	PAL	Subcortical
Anterior cingulate gyrus	ACG	Paralimbic	Thalamus	THA	Subcortical
Median cingulate gyrus	MCG	Paralimbic	Heschl gyrus	HES	Primary
Posterior cingulate gyrus	PCG	Paralimbic	Superior temporal gyrus	STG	Association
Hippocampus	HIP	Subcortical	Temporal pole (superior)	TPOsup	Paralimbic
Parahippocampal gyrus	PHG	Paralimbic	Middle temporal gyrus	MTG	Association
Amygdala	AMYG	Paralimbic	Temporal pole (middle)	TPOmid	Paralimbic
Calcarine cortex	CAL	Primary	Inferior temporal gyrus	ITG	Association
Cuneus	CUN	Association			

The brain regions were defined in terms of the automated anatomical labeling (AAL) atlas (Tzourio-Mazoyer et al. 2002)

where  $E_{global}(i)$  is derived from the neighborhood sub-network of the node  $i$ .

Regional properties of hemispheric networks were further assessed via computing nodal efficiency ( $E_{nodal}$ ).  $E_{nodal}(i)$  is defined as the inverse of the harmonic mean of the shortest path length between node  $i$  and all other nodes (Achard and Bullmore 2007):

$$E_{nodal}(i) = \frac{1}{N-1} \sum_{i \neq j \in N} \frac{1}{\min\{L_{ij}\}} \quad (5)$$

It measures the ability of node  $i$  to transmit information in the network.

We integrated the network measures over the entire sparsity range to obtain integrated global and regional network metrics (Achard and Bullmore 2007; He et al. 2008), which were used in subsequent analyses. Mathematically, these integrated metrics represent the areas under the respective metric curves.

Network hubs were further identified for both groups in terms of the normalized nodal efficiency (Tian et al. 2011):

$$\overline{E_{nodal}}(i) = \frac{N \times \sum_{s=1}^M E_{nodal}(i, s)}{\sum_{i=1}^N \sum_{s=1}^M E_{nodal}(i, s)} \quad (6)$$

where  $N$  is the number of regions (here  $N = 45$ ), and  $M$  is the number of participants in each group ( $M_{SCZ} = 66$ ,  $M_{NC} = 73$ ). A region with high normalized nodal efficiency has intense interconnectivity with other brain regions within the network. Here, region  $i$  was considered a hub of the network if  $\overline{E_{nodal}}(i)$  was at least one standard deviation above the average of the metrics.

### Asymmetry score

Brain network asymmetry of network metrics was evaluated by the asymmetry score (Iturria-Medina et al. 2011; Sun et al. 2017a, b, c):  $AS(X) = 100 \times [X(R) - X(L)]/[X(R) + X(L)]$ , where  $X(R)$  and  $X(L)$  are network parameters of the right and left hemispheres, respectively. The  $AS(X)$  index allows us to examine differences between the right and left hemispheres, with positive  $AS(X)$  indicating rightward asymmetry and negative  $AS(X)$  indicating leftward asymmetry.

### Inter-hemispheric connectivity

To examine alterations in the inter-hemispheric connectivity, the inter-hemispheric nodal strength and overall inter-

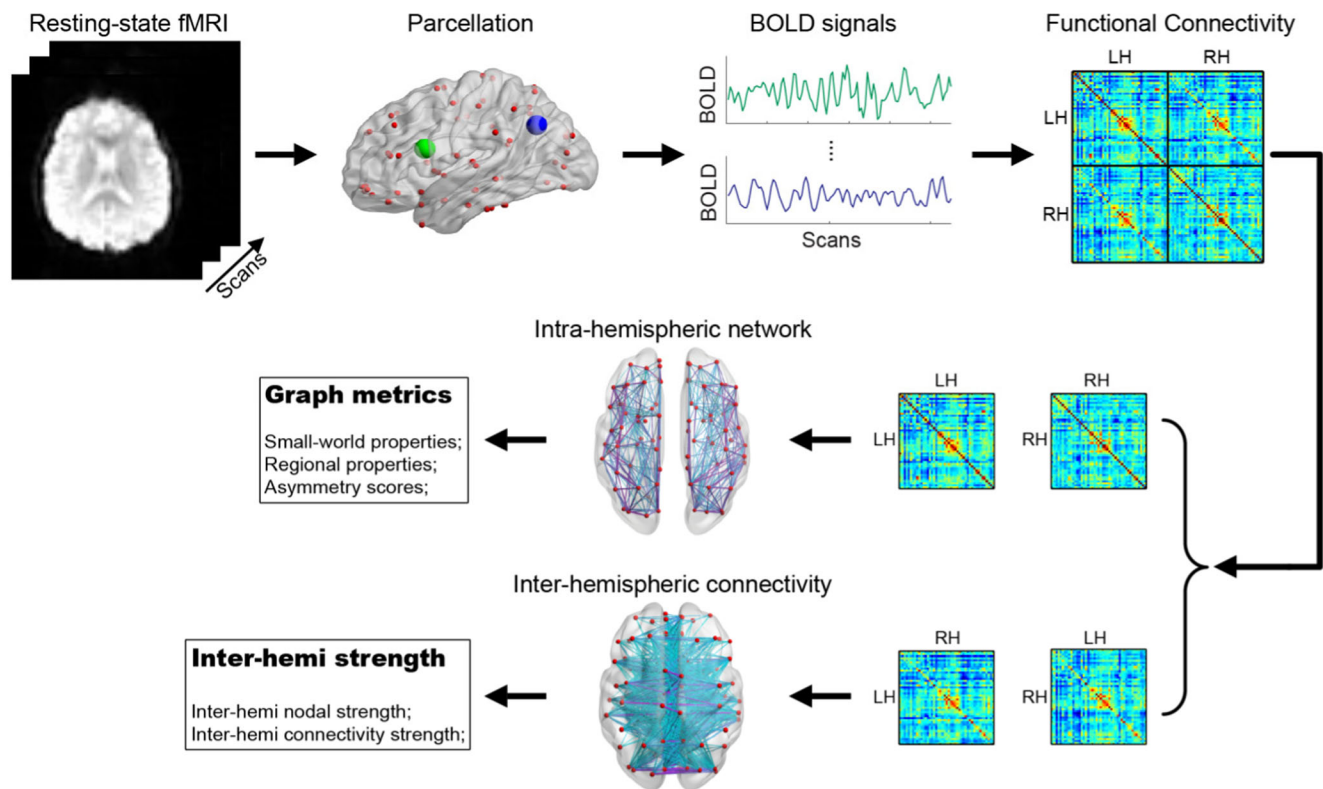


**Fig. 1 Schematic illustration of data analysis.** Resting-state fMRI data were preprocessed and the whole brain was parcellated into 90 regions of interest (ROI) in terms of the AAL template. Connectivity between all pairs of ROIs was computed and separated into intra- and inter-

hemispheric connectivity. Small-world properties, regional properties, and asymmetry scores were calculated for hemispheric networks. Inter-hemispheric nodal strength and connectivity strength were assessed. LH = left hemisphere, RH = right hemisphere

hemispheric connectivity strength were estimated. Here, the inter-hemispheric nodal strength of region  $i$  is defined as:  $Str_{Inter}(i) = \sum_{i \neq j \in Inter} e_{ij}$ , where regions  $i$  and  $j$  belong to different hemispheres and  $e_{ij}$  is the edge weight between nodes  $i$  and  $j$ . It is noteworthy that nodal strength was estimated on the original edge weight (i.e., Fisher's Z-transformed Pearson correlation coefficients) without sparsity thresholding. Of note, for a pair of regions  $i_L$  in the left hemisphere and  $i_R$  in the right hemisphere,  $Str_{Inter}(i_L)$  does not necessarily equal  $Str_{Inter}(i_R)$ . The overall inter-hemispheric connectivity strength is defined as:  $Str_{Inter} = \sum Str_{Inter}(i)/N$ .

## Statistical analysis

### Between group differences

A general linear model (GLM) was performed on the integrated network metrics to assess the hemispheric effects between two groups, with hemisphere as a within-subject factor, group as a between-subject factor, and group-by-hemisphere as the interaction. Age, gender, age-by-gender interaction, and handedness were set as covariates. In each group, a two-tailed one-sample t-test was initially used to determine whether the asymmetry score of the

network metrics was significantly different from zero. Then an ANCOVA model was applied to the asymmetry scores and inter-hemispheric connectivity to examine group differences, with age, gender and handedness as covariates. Results with  $p < 0.05$  were considered statistically significant. Multiple comparisons of nodal characteristics were corrected via false discovery rate (FDR) at  $q = 0.05$ . All statistical analyses were performed using SPSS 17 software.

### Correlations with clinical features

In the patient group, the partial correlation coefficients between clinical features and the hemispheric asymmetry scores, and between clinical features and the inter-hemispheric nodal strength, were assessed using the statistical package R (<http://www.r-project.org/>). Age, gender, age-by-gender interaction, and handedness were set as covariates. The threshold for statistical significance was set at  $p < 0.05$ . To limit the number of analyses, only brain metrics showing significant group differences were selected as independent variables in the tests of association. Corrections for multiple comparisons were not applied to the tests of association because of the exploratory nature of those analyses.

## Results

### Global properties of the hemispheric networks

#### Small-world properties

In line with previous studies (Sun et al. 2017c; Tian et al. 2011), we found that the hemispheric networks of both groups showed prominent features of small-world topology. We did not find a significant group effect or group-by-hemisphere interaction on the five global network metrics ( $ps > 0.05$ ), suggesting preserved topological properties in the hemispheric networks of patients with schizophrenia. However, a significant hemispheric effect was observed in the local efficiency (*right < left*,  $F(1, 137) = 4.528$ ,  $P = 0.035$ ), indicating a higher local communication efficiency and fault tolerance in the left hemisphere.

#### Asymmetry scores

The asymmetry scores of the five global network metrics were not significantly different from zero in the control group, while in the patient group, significant leftward advantage was observed in the asymmetry score of small-worldness ( $AS(\sigma)$ ,  $t(65) = -2.176$ ,  $p = 0.033$ ). Consistent with the GLM findings, we did not find significant group differences in the asymmetry scores of the five global network metrics.

### Regional properties of the hemispheric networks

#### Hubs

Brain regions with high nodal efficiency ( $> \text{mean} + 1\text{SD}$ ) were considered as hubs in the hemispheric networks. A hub region has intense interconnectivity with other brain regions, making it important in information transfer and integration. In healthy controls, 10 regions were identified as hubs, including 7 association (the bilateral fusiform gyrus [FFG], bilateral superior temporal gyrus [STG], bilateral middle temporal gyrus [MTG], and right inferior temporal gyrus [ITG]), 2 paralimbic (the bilateral median cingulate gyri [MCG]), and 1 primary (the left precentral gyrus [PreCG]) (Fig. 2a). In the patient group, 11 cortical regions were considered hubs, including 8 association (the bilateral FFG, bilateral STG, bilateral MTG, right ITG, and the right superior frontal gyrus, dorsal part [SFGdor]), 2 paralimbic (the left temporal pole, superior part [TPOsup] and the right insula [INS]), and 1 primary (the left PreCG) (Fig. 2a). Most of the hubs ( $n = 8$ ) overlapped between groups. It is noteworthy that most of the hemispheric network hubs are also hubs in the whole-brain network (Fig. 2b). In

particular, the identified hubs were previously reported as having high regional efficiency or betweenness centrality in structural (Bai et al. 2012; Hagmann et al. 2008; Rubinov and Bullmore 2013; Sun et al. 2017a, b, c; Wu et al. 2012) and functional (Achard and Bullmore 2007; He et al. 2009) networks. Of note, the identified hubs for both groups predominantly resided in association cortices, suggesting their importance in information transfer and integration across multiple functional systems (Mesulam 1998).

#### Hemispheric and group effects

Significant hemispheric effects ( $p < 0.05$ , FDR-corrected) were observed in 10 brain regions, where four regions (the angular gyrus [ANG], insula [INS], cuneus [CUN], and superior temporal gyrus [STG]) showed rightward predilection and the remaining six regions (the inferior parietal lobe [IPL], posterior cingulate gyrus [PCG], precuneus [PCUN], precentral gyrus [PreCG], superior frontal gyrus, medial part [SFGmed], and middle occipital gyrus [MOG]) exhibited a leftward advantage in regional efficiency (Fig. 3 and Table 3). Furthermore, a significant group effect ( $p < 0.05$ , FDR-corrected) was revealed in five brain regions (the median cingulate gyrus [MCG], hippocampus [HIP], pallidum [PAL], putamen [PUT], and thalamus [THA]). Specifically, patients showed decreased efficiency in the MCG and increased efficiency in the other four subcortical regions. Moreover, a significant group-by-hemisphere interaction was revealed in the temporal pole, middle part [TPomid], ( $F(1, 137) = 16.082$ ,  $p = 9.92 \times 10^{-5}$ ). Post-hoc analysis further revealed a rightward advantage of nodal efficiency in healthy controls ( $t(72) = -3.407$ ,  $p = 0.001$ ) and a leftward predilection in patients ( $t(65) = 2.310$ ,  $p = 0.024$ ).

#### Asymmetry scores

In healthy controls, the efficiency of seven brain regions showed significant asymmetry ( $p < 0.05$ , FDR-corrected). Among these regions, three of them (the MOG, IPL, and orbitofrontal gyrus [ORBinf]) exhibited a leftward preference, whereas the remaining four regions (the CUN, ANG, INS, and STG) showed a rightward advantage. No significant asymmetry in regional efficiency was found ( $p > 0.05$ , FDR-corrected) in the patient group. We further examined group differences in regional asymmetry scores and found a trend for a group difference in the TPomid ( $F(1, 132) = 8.324$ ,  $p = 0.005$ ), consistent with the significant group-by-hemispheric interaction revealed in the GLM.

#### Inter-hemispheric connectivity

The inter-hemispheric nodal strength is presented in Fig. 4. Statistical analysis revealed a significant deficit ( $p < 0.05$ ,

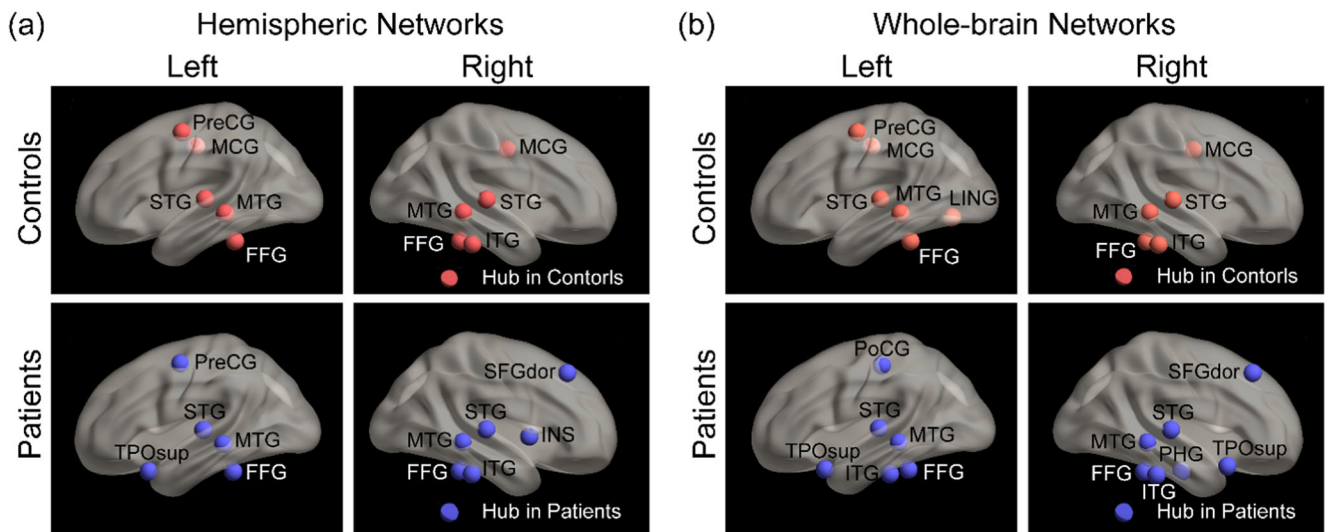


**Fig. 2 Hubs in healthy controls and patients with schizophrenia.** **a** Ten regions were identified as hemispheric hubs in healthy controls and 11 regions were identified as hubs in the patient group. Most of the hubs

resided in association cortices and overlapped across groups. **b** Hemispheric hubs were also identified as hubs in the whole brain network

FDR-corrected) in the inter-hemispheric connectivity of most brain regions (left hemisphere, 24/45; right hemisphere, 25/45), leading to an overall hypo-connectivity between the two hemispheres in patients ( $F(1, 132) = 7.231, p = 0.008$ ). Further inspection of the inter-hemispheric dysconnectivity pattern revealed that significant deficits mainly resided in association cortices, which were identified as hubs (Fig. 2) in this and in previous studies (Achard et al. 2006; Rubinov and Bullmore 2013).

### Correlations with clinical features

We assessed the correlation between regional asymmetry scores and clinical features. We found that  $AS(E_{nodal}(IPL))$  was negatively correlated with the disease duration ( $r = -0.262, p = 0.033$ );  $AS(E_{nodal}(PUT))$  was positively correlated with the PANSS positive symptoms ( $r = 0.254, p = 0.040$ ), general symptoms ( $r = 0.292, p = 0.017$ ), and overall symptoms ( $r = 0.329, p = 0.007$ ); and  $AS(E_{nodal}(STG))$  was negatively correlated with the PANSS general symptoms ( $r = -0.267, p = 0.030$ ) and disease duration ( $r = -0.264, p = 0.032$ ) (Table 4). We further examined the correlations between inter-hemisphere connectivity and clinical features. We found that the PANSS positive score was positively correlated with  $Str_{Inter}$  in the FFG<sub>L</sub>, PCUN<sub>L</sub>, SFGmed<sub>R</sub>, SOG<sub>R</sub>, PCL<sub>R</sub>, and STG<sub>R</sub>; the PANSS general score was positively correlated with  $Str_{Inter}$  in the PCL<sub>R</sub> and STG<sub>R</sub>; the PANSS overall score was positively correlated with  $Str_{Inter}$  in the SFGmed<sub>R</sub>, PCL<sub>R</sub>, and STG<sub>R</sub>; and the PANSS negative score was negatively correlated with the  $Str_{Inter}$  in SOG<sub>R</sub> (Table 4).

### Discussion

In this study, we investigated the source of functional dysconnectivity in schizophrenia by combining resting-state fMRI and graph theoretical analysis. We found that schizophrenia-related alterations occurred only in regional characteristics. The global network topology of hemispheric networks was intact in patients, as in the healthy controls. Moreover, we observed an overall hypo-connectivity between the left and right hemispheres in patients, which was attributed to deficits in the inter-hemispheric connectivity of brain regions mainly in the association cortices. Furthermore, we found that the abnormalities in intra- and inter-hemispheric network properties were correlated with the clinical features of schizophrenia. These findings are discussed below in detail.

Small-world architecture, which has been identified at the whole-brain level in both healthy individuals and patients with schizophrenia (Bullmore and Sporns 2009; Fornito et al. 2012; van den Heuvel and Fornito 2014), was recently found in the hemispheric functional (Tian et al. 2011) and structural (Iturria-Medina et al. 2011; Sun et al. 2017a, c) networks. Consistent with these previous findings, we found that small-world properties were preserved in the hemispheric functional networks in schizophrenia, demonstrating that the efficiency of information processing within each hemisphere could be similar to that in the whole brain (Tian et al. 2011). Moreover, a significant hemispheric effect was observed on local efficiency, showing a leftward advantage in local information processing. This finding is in line with the notion that there is a more internal communication in the left hemisphere

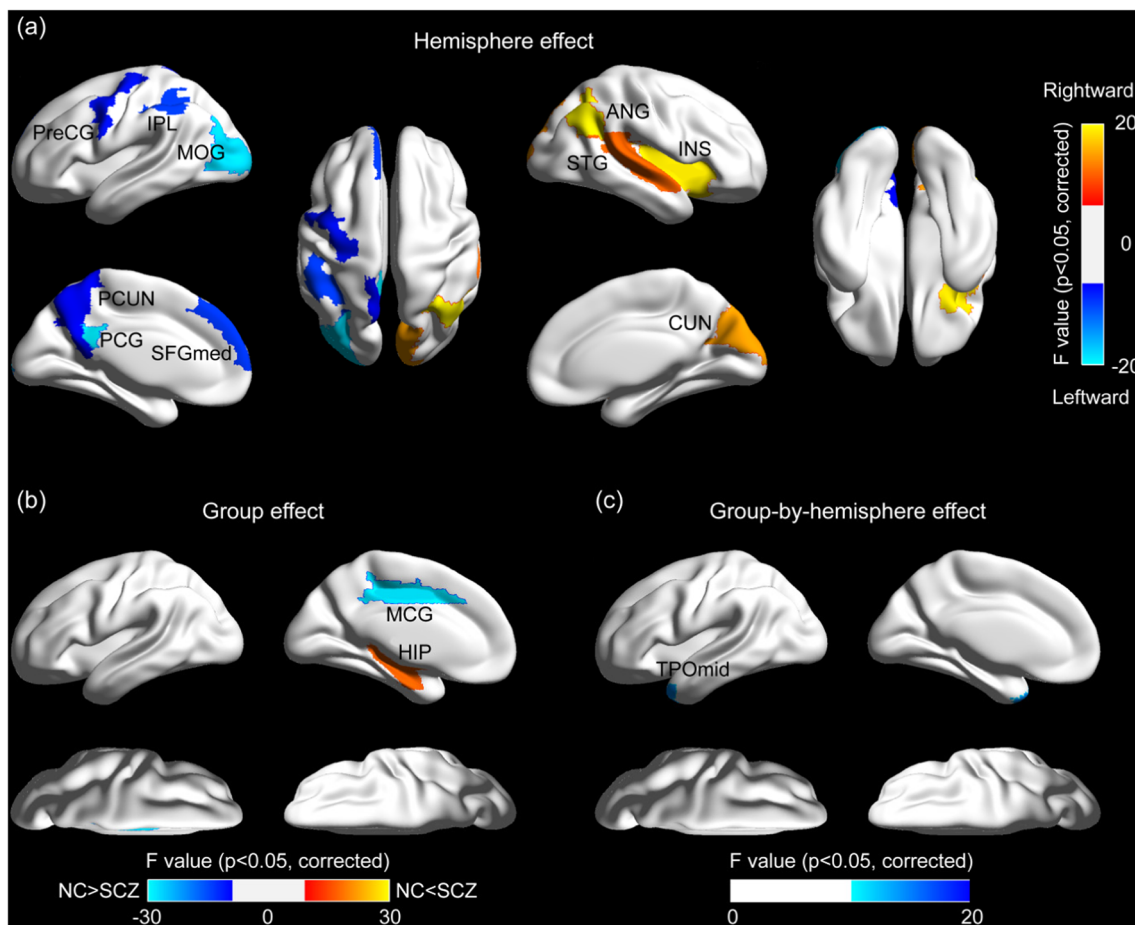


**Fig. 3** The surface spatial distribution of cortical regions showing significant effects ( $p < 0.05$ , FDR corrected). **a** Hemispheric effect was observed in 10 brain regions, with 4 regions showing rightward predilection and the remaining 6 regions showing leftward advantage in regional efficiency. **b** Group effect was observed in 5 brain regions, with patients showing decreased efficiency in the middle cingulate and increased efficiency in subcortical regions. Note: subcortical regions

showing significant group effect (including the PUT, THA, and PAL) were not presented in the surface spatial distribution. **c** Group-by-hemispheric interaction was observed in the middle temporal pole, with a rightward advantage in healthy controls and a leftward predilection in patients. The colored bar represents F-values. Significant regions are overlaid on inflated surface using BrainNet Viewer (Xia et al. 2013)

and a more integrative communication with both hemispheres in the right hemisphere (Gotts et al. 2013).

In contrast to previous studies that reported significant alterations in global network properties in schizophrenia (Fornito et al. 2012; van den Heuvel and Fornito 2014), we did not find any significant group effect on global properties. The discrepancy may arise from the fact that previous studies exclusively examined the “whole-brain” network whereas this study examined the hemispheric networks. Furthermore, in the current study we did not find a group difference in the hemispheric asymmetry of global network properties, although in other recent work we did find reduced hemispheric asymmetry of structural network properties in patients with schizophrenia (Sun et al. 2017a). The divergence may be attributed to the complex relationship between structural and functional connectivity in healthy individuals and in patients with schizophrenia (Damoiseaux and Greicius 2009; Z. Wang et al. 2015; Cocchi et al. 2014; Skudlarski et al. 2010;

Sun et al. 2017b; van den Heuvel et al. 2013). For example, while structural connectivity was uniformly lower in schizophrenia, functional connectivity in schizophrenia was lower in some connections and higher in others, which could reflect either a dysregulation of neural activities or a compensation for primary deficits (Fornito et al. 2012). In line with this notion, we found that schizophrenia-related aberrations of association between structural and functional connectivity exhibited complex patterns among different functional modules (Sun et al. 2017b). Given the paucity of research on schizophrenia-related connectome disruption in hemispheric networks, further studies may help to reconcile the inconsistencies.

We further examined group differences in regional characteristics of hemispheric networks. We found that schizophrenia was associated with increased regional efficiency in subcortical areas and decreased efficiency in the cingulate gyrus. Abnormalities of the subcortical nuclei and cingulate cortex have been consistently reported in schizophrenia

**Table 3** Group and hemispheric effects on the nodal efficiency

Region	Classification	General linear model		
		Group effect $F_{1,132}$ ( $p$ -value)	Hemisphere effect $F_{1,137}$ ( $p$ -value)	Interaction $F_{1,137}$ ( $p$ -value)
ANG	Association	3.518 (0.063)	<b>19.610 (1.93E<sup>-05</sup>)</b> <	0.466 (0.496)
CUN	Association	4.935 (0.028)	<b>15.099 (1.58E<sup>-04</sup>)</b> <	1.524 (0.219)
MCG	Paralimbic	<b>27.941 (5.04E<sup>-07</sup>)</b> †	3.784 (0.0538)	0.739 (0.392)
HIP	Subcortical	<b>17.318 (5.67E<sup>-05</sup>)</b> ↓	3.223 (0.0748)	1.563 (0.213)
INS	Paralimbic	1.557 (0.214)	<b>19.005 (2.54E<sup>-05</sup>)</b> <	0.612 (0.435)
IPL	Association	2.131 (0.147)	<b>9.733 (0.002)</b> >	1.451 (0.230)
MOG	Association	0.815 (0.368)	<b>18.369 (3.41E<sup>-05</sup>)</b> >	0.00727 (0.932)
PAL	Subcortical	<b>9.284 (0.00279)</b> ↓	2.742 (0.100)	4.797 (0.0302)
PCG	Paralimbic	0.00319 (0.955)	<b>19.113 (2.42E<sup>-05</sup>)</b> >	1.122 (0.291)
PCUN	Association	2.009 (0.159)	<b>6.775 (0.0103)</b> >	0.743 (0.390)
PreCG	Primary	0.599 (0.440)	<b>7.32 (0.00768)</b> >	0.0192 (0.890)
PUT	Subcortical	<b>29.362 (2.76E<sup>-07</sup>)</b> ↓	0.124 (0.725)	0.0960 (0.329)
SFGmed	Association	0.330 (0.567)	<b>9.619 (0.00234)</b> >	0.0196 (0.889)
STG	Association	6.835 (0.00998)	<b>11.945 (0.000730)</b> <	1.816 (0.180)
THA	Subcortical	<b>22.608 (5.13E<sup>-06</sup>)</b> ↓	0.260 (0.611)	3.600 (0.0599)
TPOmid	Paralimbic	0.576 (0.449)	0.339 (0.562)	<b>16.082 (9.92E<sup>-05</sup>)</b>

General Linear Model was employed to examine the hemisphere effect, group effect, and hemisphere-by-group interaction, with age, gender, and age-by-gender as covariates. Subject was entered as random effect. Significant effects ( $p < 0.05$ , FDR corrected) were indicated by bold and shaded text. Refer to Table 2 for the abbreviations of brain regions. Note: >, left > right; <, left < right; †, NC > SCZ; ↓ NC < SCZ

(Alexander-Bloch et al. 2010; Fornito et al. 2011; Fornito et al. 2012; Y. Liu et al. 2008; Lynall et al. 2010). In particular, the association between pathology of subcortical regions and various clinical manifestations in the pathogenesis of schizophrenia has already been recognized (Rimol et al. 2010). In a recent multisite study of subcortical brain aberrations in 2028 patients with schizophrenia, significantly reduced volume of subcortical regions was reported (van Erp et al. 2016). In terms of connectivity characteristics, subcortical regions such as striatum were linked with increased regional strength (Y. Liu et al. 2008; Salvador et al. 2010) whereas cingulate cortex was linked with decreased regional strength (Lynall et al. 2010). Consistent with these studies, our findings therefore further suggest aberrant centrality of paralimbic vs. subcortical regions in information propagations in schizophrenia. Additionally, a significant group-by-hemisphere interaction was found in the middle temporal pole, which exhibited a leftward advantage in patients and a rightward predilection in healthy controls. Given that the temporal pole is located close to the orbitofrontal cortex and amygdala and connects tightly with the limbic/paralimbic regions, it is believed to play an important role in binding various perceptual inputs to visceral emotional responses (Olson et al. 2007). In fact, dysfunction of the temporal pole has been linked with diseases that involve deficits in socio-emotional processing (Olson et al. 2007), such as schizophrenia (Crespo-Facorro et al. 2004; Gur et al. 2000; Kasai et al. 2003) and semantic dementia (Thompson et al. 2003).

Our observations extend previous findings by linking schizophrenia with aberrant asymmetry of the efficiency of information exchange in the temporal pole.

Furthermore, inter-hemispheric deficits were found in most brain regions (S. Guo et al. 2013; W. Guo et al. 2014; Hoptman et al. 2012), leading to an overall hypo-connectivity between the two hemispheres. Specifically, most of these aberrant regions were association cortical hubs. Of note, the identified hemispheric hubs have been repeatedly reported as hubs at the whole-brain (Bassett et al. 2012; Rubinov and Bullmore 2013) and hemispheric (Sun et al. 2017a, b, c; Tian et al. 2011) level, indicating their importance in both intra- and inter-hemispheric information exchanges. Previous studies have found abnormalities in the frontal, temporal, and parietal association cortical hubs at the whole-brain level (Alexander-Bloch et al. 2013; Bassett et al. 2012; Rubinov and Bullmore 2013; L. Wang et al. 2010). Our observations further extend these findings in that abnormalities in hubs may predominantly result from deficits in the inter-hemispheric connections. More importantly, our findings showing preserved intra-hemispheric network topology and impaired inter-hemispheric connectivity in patients demonstrate that the dysconnection results from inter- rather than intra-hemispheric deficits.

In addition, we found that the asymmetry of hemispheric network properties was associated with patients' symptom severity. Specifically, symptom severity increased with decreasing asymmetry of superior temporal efficiency,

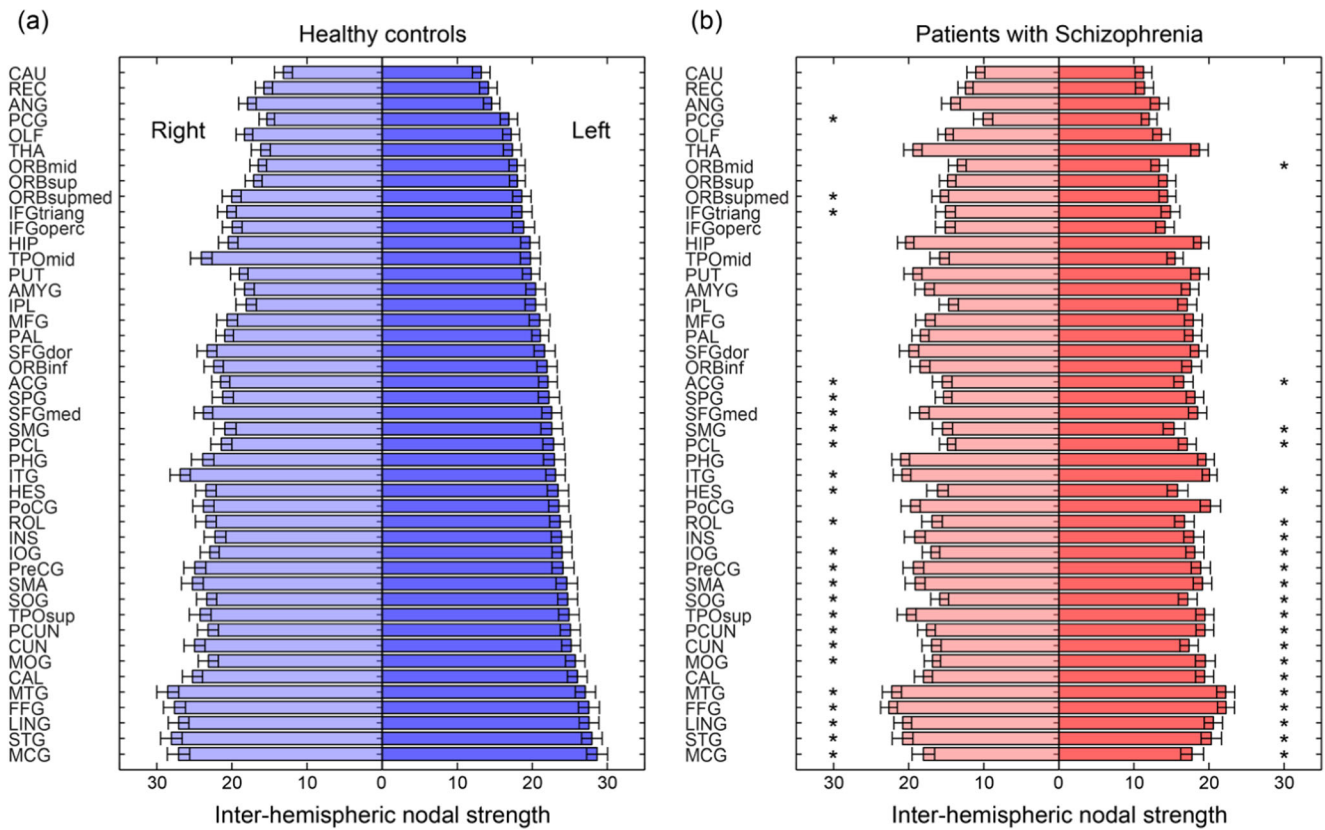


**Fig. 4** Inter-hemisphere nodal strength in healthy controls and patients with schizophrenia. **a** Brain regions were sorted in ascending order of nodal strength in the left hemisphere in healthy controls. **b** Deficits existed in the inter-hemispheric connectivity of most brain

regions, leading to an overall hypo-connectivity between the two hemispheres in patients. Regions with significant group differences ( $p < 0.05$ , FDR corrected) are highlighted

consistent with previous findings of a negative correlation between symptom severity and lateralization of language processing areas (Artiges et al. 2000; Sommer et al. 2001).

Moreover, symptom severity increased with increasing asymmetry of subcortical efficiency, providing evidence for the dopamine hypothesis that subcortical hyperdopaminergic

**Table 4** Association between network measures and clinical features in patients with schizophrenia

Metrics	Partial correlation coefficients ( $P$ -value)				
	PANSS positive	PANSS negative	PANSS general	PANSS overall	Duration
<b>Asymmetry scores</b>					
$AS(E_{nodal}(IPL))$	-0.102 (0.416)	-0.165 (0.184)	-0.183 (0.141)	-0.199 (0.109)	<b>-0.262 (0.033)</b>
$AS(E_{nodal}(PUT))$	<b>0.254 (0.040)</b>	0.209 (0.093)	<b>0.292 (0.017)</b>	<b>0.329 (0.007)</b>	-0.170 (0.174)
$AS(E_{nodal}(STG))$	-0.116 (0.354)	-0.005 (0.965)	<b>-0.267 (0.030)</b>	-0.202 (0.104)	<b>-0.264 (0.032)</b>
<b>Inter-hemispheric connectivity strength</b>					
$Str_{inter}(FFG_L)$	<b>0.275 (0.024)</b>	0.015 (0.901)	0.215 (0.080)	0.230 (0.061)	-0.008 (0.947)
$Str_{inter}(PCUN_L)$	<b>0.273 (0.026)</b>	0.001 (0.995)	0.225 (0.067)	0.230 (0.061)	-0.034 (0.782)
$Str_{inter}(SFGmed_R)$	<b>0.246 (0.045)</b>	0.165 (0.181)	0.193 (0.118)	<b>0.257 (0.035)</b>	0.115 (0.210)
$Str_{inter}(SOG_R)$	-0.041 (0.744)	<b>-0.263 (0.031)</b>	-0.155 (0.210)	-0.199 (0.107)	-0.129 (0.298)
$Str_{inter}(PCL_R)$	<b>0.257 (0.036)</b>	-0.001 (0.991)	<b>0.269 (0.028)</b>	<b>0.250 (0.041)</b>	0.121 (0.328)
$Str_{inter}(STG_R)$	<b>0.260 (0.034)</b>	0.150 (0.225)	<b>0.249 (0.042)</b>	<b>0.291 (0.017)</b>	-0.015 (0.905)

The partial correlations between network measures and clinical features were estimated with age, gender, age-by-gender interaction, and handedness as covariates. Significant correlation ( $p < 0.05$ ) is indicated by bolded text. Refer to Table 2 for the abbreviations of brain regions. The positive and negative syndrome scale (PANSS) was used to assess psychopathology and symptom severity (Kay et al. 1987). L = left, R = right

function plays a central role in schizophrenia (Stephan et al. 2009). As mentioned before, pathology of subcortical regions has long been linked to the pathogenesis of schizophrenia and various clinical manifestations (Hoffman et al. 2011). Moreover, we found that the inter-hemispheric connectivity was associated with symptom severity in patients. Specifically, severity of positive symptoms increased with increasing inter-hemispheric connectivity in the right frontal and bilateral temporal cortices, whereas severity of negative symptoms increased with decreasing inter-hemispheric connectivity in the right occipital cortex. Positive psychotic symptoms of schizophrenia typically encompass hallucinations and delusions (Howes and Murray 2014).

In line with our findings, previous imaging studies of psychotic symptoms have reported diminished lateralization of temporal regions in those who have auditory hallucinations compared with those who do not (Collinson et al. 2009) and predominantly right hemispheric activation during auditory hallucinations (Sommer et al. 2001). In the occipital cortex, significant reductions of resting-state functional connectivity (H. Liu et al. 2006) and gray matter density (Ananth et al. 2002) have been widely revealed in schizophrenia, indicating impairment of early cortical processing involving the visual cortex (Butler et al. 2008). Together, these findings suggest that connectivity properties could be potential biomarkers for diagnosis of schizophrenia and assessment of symptom severity. Notwithstanding, the association results were assessed without corrections for multiple comparisons and the findings should be interpreted as exploratory in nature. Further studies with independent samples are recommended to confirm our observations.

Several methodological issues should be taken into consideration while interpreting the current results. First, while previous studies found that diverse antipsychotic medication statuses in patients with schizophrenia may affect brain activities in localized regions and connections (Navari and Dazzan 2009), findings regarding the association between medication statuses and network properties are inconsistent (Y. Liu et al. 2008; Ribolsi et al. 2009). Actually, Rubinov and colleagues suggested that medication may exert a normalizing rather than confounding influence (Rubinov et al. 2009). Altered functional connectivity reported in schizophrenia was also found in patients' unaffected siblings (Collin et al. 2014; Repovs et al. 2011), suggesting that inherited susceptibility to schizophrenia and intrinsic components of its pathophysiology may be captured by abnormalities in at least some functional connections. Therefore, we believe that our current finding of group differences may result from the intrinsic disease process rather than direct pharmacological treatment. Second, the AAL template was used to construct the brain network. The anatomical boundaries of nodes in the AAL template may not well match functional boundaries, and a relatively large number of anatomical nodes might contain heterogeneous signals

that further influence the network construction (Smith et al. 2011). However, the primary focus of this study was to investigate the complex nature of dysconnection in terms of intra- and inter-hemispheric connectivity patterns. As most findings in the field were established on the AAL template, we chose to use the same template to enable direct comparisons with most previous studies. Furthermore, Arslan and colleagues systematically compared different parcellation methods and found no optimal method in terms of simultaneously addressing all challenges (Arslan et al. 2017). Therefore, examining schizophrenia-related alterations across multiple resolutions may be important to validate our observations. Third, previous connectivity studies suggested that high global integration assures effective integrity or rapid transfers of information across remote regions that are believed to constitute the basis of cognitive processing (Sporns and Zwi 2004). More recently, van den Heuvel and colleagues showed that efficiency of functional brain networks in non-patients is associated with intellectual performance (van den Heuvel et al. 2009), which was also found to be the case for intelligence prediction (Langer et al. 2012). Meanwhile, an association between low intelligence quotient and schizophrenia has been repeatedly reported (e.g. (David et al. 1997)). To account for the potential influence of a significant between-group difference in cognitive abilities, we performed additional statistical analysis (i.e., separate GLMs for intra- and inter-hemispheric network metrics as well as new partial correlation models for association analysis) where education and WAIS sum were set as covariates together with previous covariates (age, gender, age-by-gender, and handedness), and we found the main observations intact (data not shown). However, the inclusion of medicated patients in the current work makes it hard to exclude the possibility that the disorder itself or disease management (i.e., pharmacological treatment) leads to a decline in IQ. Further studies with drug-naïve patients are therefore of interest to confirm our observations. Finally, recent studies found frequency-specific alterations in functional connectivity in schizophrenia (X. Wang et al. 2017; R. Yu et al. 2014). Future research may further explore the relation between frequency bands (e.g., slow-4 (0.027–0.073 Hz) vs. slow-5 (0.01–0.027 Hz)) and dysconnectivity in schizophrenia.

In conclusion, the current study examined the source of functional dysconnectivity in schizophrenia. We found that small-world properties and lateralization of global network properties are preserved in patients. Schizophrenia-related alterations occurred only in subcortical and cingulate efficiency and inter-hemispheric interactions between hub regions. The abnormalities of intra- and inter-hemispheric properties were associated with clinical features. Taken together, these findings suggest that inter- but not intra-hemispheric dysconnectivity may underlie altered brain functions and clinical symptoms observed in schizophrenia.

## Compliance with ethical standards

**Conflict of interest** The authors have nothing to disclose.

**Sources of support** This work was supported by Zhejiang University (“Hundred Talents Program” awarded to Y. S.), by the Fundamental Research Funds for the Central Universities (Grant no. 2018QNA5017 awarded to Y.S.), and by the Ministry of Education of Singapore (MOE2016-T2-1-015 awarded to R. Y.). The funders had no role in study design, data collection and analysis, decision to publish, or preparation of the manuscript.

**Informed consent** All procedures followed were in accordance with the ethical standards of the responsible committee on human experimentation (institutional and national) and with the Helsinki Declaration of 1975, and the applicable revisions at the time of the investigation. Informed consent was obtained from all patients included in the study.

## References

- Achard, S., & Bullmore, E. (2007). Efficiency and cost of economical brain functional networks. *PLoS Computational Biology*, 3(2), e17. <https://doi.org/10.1371/journal.pcbi.0030017>.
- Achard, S., Salvador, R., Whitcher, B., Suckling, J., & Bullmore, E. (2006). A resilient, low-frequency, small-world human brain functional network with highly connected association cortical hubs. *The Journal of Neuroscience*, 26(1), 63–72. <https://doi.org/10.1523/JNEUROSCI.3874-05.2006>.
- Alexander-Bloch, A. F., Gogtay, N., Meunier, D., Birn, R., Clasen, L., Lalonde, F., Lenroot, R., Giedd, J., & Bullmore, E. T. (2010). Disrupted modularity and local connectivity of brain functional networks in childhood-onset schizophrenia. *Frontiers in Systems Neuroscience*, 4, 147. <https://doi.org/10.3389/fnsys.2010.00147>.
- Alexander-Bloch, A. F., Vertes, P. E., Stidd, R., Lalonde, F., Clasen, L., Rapoport, J., et al. (2013). The anatomical distance of functional connections predicts brain network topology in health and schizophrenia. *Cerebral Cortex*, 23(1), 127–138. <https://doi.org/10.1093/cercor/bhr388>.
- Ananth, H., Popescu, I., Critchley, H. D., Good, C. D., Frackowiak, R. S., & Dolan, R. J. (2002). Cortical and subcortical gray matter abnormalities in schizophrenia determined through structural magnetic resonance imaging with optimized volumetric voxel-based morphometry. *The American Journal of Psychiatry*, 159(9), 1497–1505. <https://doi.org/10.1176/appi.ajp.159.9.1497>.
- Anderson, J. S., Druzgal, T. J., Lopez-Larson, M., Jeong, E. K., Desai, K., & Yurgelun-Todd, D. (2011). Network anticorrelations, global regression, and phase-shifted soft tissue correction. *Human Brain Mapping*, 32(6), 919–934. <https://doi.org/10.1002/hbm.21079>.
- Arslan, S., Ktena, S. I., Makropoulos, A., Robinson, E. C., Rueckert, D., & Parisot, S. (2017). Human brain mapping: A systematic comparison of parcellation methods for the human cerebral cortex. *Neuroimage*, 170, 5–30. <https://doi.org/10.1016/j.neuroimage.2017.04.014>.
- Artiges, E., Martinot, J. L., Verdys, M., Attar-Levy, D., Mazoyer, B., Tzourio, N., Giraud, M. J., & Paillere-Martinot, M. L. (2000). Altered hemispheric functional dominance during word generation in negative schizophrenia. *Schizophrenia Bulletin*, 26(3), 709–721.
- Bai, F., Shu, N., Yuan, Y., Shi, Y., Yu, H., Wu, D., Wang, J., Xia, M., He, Y., & Zhang, Z. (2012). Topologically convergent and divergent structural connectivity patterns between patients with remitted geriatric depression and amnesic mild cognitive impairment. *The Journal of Neuroscience*, 32(12), 4307–4318. <https://doi.org/10.1523/JNEUROSCI.5061-11.2012>.
- Bassett, D. S., Nelson, B. G., Mueller, B. A., Camchong, J., & Lim, K. O. (2012). Altered resting state complexity in schizophrenia. *Neuroimage*, 59(3), 2196–2207. <https://doi.org/10.1016/j.neuroimage.2011.10.002>.
- Bleich-Cohen, M., Hendler, T., Kotler, M., & Strous, R. D. (2009). Reduced language lateralization in first-episode schizophrenia: An fMRI index of functional asymmetry. *Psychiatry Research*, 171(2), 82–93. <https://doi.org/10.1016/j.psychres.2008.03.002>.
- Bullmore, E., & Sporns, O. (2009). Complex brain networks: Graph theoretical analysis of structural and functional systems. *Nature Reviews Neuroscience*, 10(3), 186–198. <https://doi.org/10.1038/nrn2575>.
- Butler, P. D., Silverstein, S. M., & Dakin, S. C. (2008). Visual perception and its impairment in schizophrenia. *Biological Psychiatry*, 64(1), 40–47. <https://doi.org/10.1016/j.biopsych.2008.03.023>.
- Cocchi, L., Harding, I. H., Lord, A., Pantelis, C., Yucel, M., & Zalesky, A. (2014). Disruption of structure-function coupling in the schizophrenia connectome. *Neuroimage Clinical*, 4, 779–787. <https://doi.org/10.1016/j.nicl.2014.05.004>.
- Collin, G., Kahn, R. S., de Reus, M. A., Cahn, W., & van den Heuvel, M. P. (2014). Impaired rich club connectivity in unaffected siblings of schizophrenia patients. *Schizophrenia Bulletin*, 40(2), 438–448. <https://doi.org/10.1093/schbul/sbt162>.
- Collinson, S. L., Mackay, C. E., O, J., James, A. C., & Crow, T. J. (2009). Dichotic listening impairments in early onset schizophrenia are associated with reduced left temporal lobe volume. *Schizophrenia Research*, 112(1–3), 24–31. <https://doi.org/10.1016/j.schres.2009.03.034>.
- Crespo-Facorro, B., Nopoulos, P. C., Chemerinski, E., Kim, J. J., Andreasen, N. C., & Magnotta, V. (2004). Temporal pole morphology and psychopathology in males with schizophrenia. *Psychiatry Research*, 132(2), 107–115. <https://doi.org/10.1016/j.psychres.2004.09.002>.
- Damoiseaux, J. S., & Greicius, M. D. (2009). Greater than the sum of its parts: A review of studies combining structural connectivity and resting-state functional connectivity. *Brain Structure & Function*, 213(6), 525–533. <https://doi.org/10.1007/s00429-009-0208-6>.
- David, A. S., Malmberg, A., Brandt, L., Allebeck, P., & Lewis, G. (1997). IQ and risk for schizophrenia: A population-based cohort study. *Psychological Medicine*, 27(6), 1311–1323.
- Ellison-Wright, I., & Bullmore, E. (2009). Meta-analysis of diffusion tensor imaging studies in schizophrenia. *Schizophrenia Research*, 108(1–3), 3–10. <https://doi.org/10.1016/j.schres.2008.11.021>.
- Fornito, A., Yoon, J., Zalesky, A., Bullmore, E. T., & Carter, C. S. (2011). General and specific functional connectivity disturbances in first-episode schizophrenia during cognitive control performance. *Biological Psychiatry*, 70(1), 64–72. <https://doi.org/10.1016/j.biopsych.2011.02.019>.
- Fornito, A., Zalesky, A., Pantelis, C., & Bullmore, E. T. (2012). Schizophrenia, neuroimaging and connectomics. *Neuroimage*, 62(4), 2296–2314. <https://doi.org/10.1016/j.neuroimage.2011.12.090>.
- Fox, M. D., & Raichle, M. E. (2007). Spontaneous fluctuations in brain activity observed with functional magnetic resonance imaging. *Nature Reviews Neuroscience*, 8(9), 700–711. <https://doi.org/10.1038/nrn2201>.
- Friston, K., Brown, H. R., Siemerkus, J., & Stephan, K. E. (2016). The dysconnection hypothesis (2016). *Schizophrenia Research*, 176(2–3), 83–94. <https://doi.org/10.1016/j.schres.2016.07.014>.
- Gotts, S. J., Jo, H. J., Wallace, G. L., Saad, Z. S., Cox, R. W., & Martin, A. (2013). Two distinct forms of functional lateralization in the human brain. *Proceedings of the National Academy of Sciences of the United States of America*, 110(36), E3435–E3444. <https://doi.org/10.1073/pnas.1302581110>.
- Guo, S., Kendrick, K. M., Zhang, J., Broome, M., Yu, R., Liu, Z., & Feng, J. (2013). Brain-wide functional inter-hemispheric disconnection is

- a potential biomarker for schizophrenia and distinguishes it from depression. *Neuroimage Clinical*, 2, 818–826. <https://doi.org/10.1016/j.nicl.2013.06.008>.
- Guo, W., Xiao, C., Liu, G., Wooderson, S. C., Zhang, Z., Zhang, J., Yu, L., & Liu, J. (2014). Decreased resting-state interhemispheric coordination in first-episode, drug-naive paranoid schizophrenia. *Progress in Neuro-Psychopharmacology & Biological Psychiatry*, 48, 14–19. <https://doi.org/10.1016/j.pnpbp.2013.09.012>.
- Gur, R. E., Turetsky, B. I., Cowell, P. E., Finkelman, C., Maany, V., Grossman, R. I., Arnold, S. E., Bilker, W. B., & Gur, R. C. (2000). Temporolimbic volume reductions in schizophrenia. *Archives of General Psychiatry*, 57(8), 769–775.
- Hagmann, P., Cammoun, L., Gigandet, X., Meuli, R., Honey, C. J., Wedeen, V. J., & Sporns, O. (2008). Mapping the structural core of human cerebral cortex. *PLoS Biology*, 6(7), e159. <https://doi.org/10.1371/journal.pbio.0060159>.
- He, Y., & Evans, A. (2010). Graph theoretical modeling of brain connectivity. *Current Opinion in Neurology*, 23(4), 341–350. <https://doi.org/10.1097/WCO.0b013e32833aa567>.
- He, Y., Chen, Z., & Evans, A. (2008). Structural insights into aberrant topological patterns of large-scale cortical networks in Alzheimer's disease. *The Journal of Neuroscience*, 28(18), 4756–4766. <https://doi.org/10.1523/JNEUROSCI.0141-08.2008>.
- He, Y., Wang, J., Wang, L., Chen, Z. J., Yan, C., Yang, H., Tang, H., Zhu, C., Gong, Q., Zang, Y., & Evans, A. C. (2009). Uncovering intrinsic modular organization of spontaneous brain activity in humans. *PLoS One*, 4(4), e5226. <https://doi.org/10.1371/journal.pone.0005226>.
- Hoffman, R. E., Fernandez, T., Pittman, B., & Hampson, M. (2011). Elevated functional connectivity along a corticostriatal loop and the mechanism of auditory/verbal hallucinations in patients with schizophrenia. *Biological Psychiatry*, 69(5), 407–414. <https://doi.org/10.1016/j.biopsych.2010.09.050>.
- Honey, C. J., Sporns, O., Cammoun, L., Gigandet, X., Thiran, J. P., Meuli, R., & Hagmann, P. (2009). Predicting human resting-state functional connectivity from structural connectivity. *Proceedings of the National Academy of Sciences of the United States of America*, 106(6), 2035–2040. <https://doi.org/10.1073/pnas.0811168106>.
- Hoptman, M. J., Zuo, X. N., D'Angelo, D., Mauro, C. J., Butler, P. D., Milham, M. P., & Javitt, D. C. (2012). Decreased interhemispheric coordination in schizophrenia: A resting state fMRI study. *Schizophrenia Research*, 141(1), 1–7. <https://doi.org/10.1016/j.schres.2012.07.027>.
- Howes, O. D., & Murray, R. M. (2014). Schizophrenia: an integrated sociodevelopmental-cognitive model. *Lancet*, 383(9929), 1677–1687. [https://doi.org/10.1016/S0140-6736\(13\)62036-X](https://doi.org/10.1016/S0140-6736(13)62036-X).
- Humphries, M. D., Gurney, K., & Prescott, T. J. (2006). The brainstem reticular formation is a small-world, not scale-free, network. *Proceedings of the Biological Sciences*, 273(1585), 503–511. <https://doi.org/10.1098/rspb.2005.3354>.
- Iturria-Medina, Y., Perez Fernandez, A., Morris, D. M., Canales-Rodriguez, E. J., Haroon, H. A., Garcia Penton, L., et al. (2011). Brain hemispheric structural efficiency and interconnectivity rightward asymmetry in human and nonhuman primates. *Cerebral Cortex*, 21(1), 56–67. <https://doi.org/10.1093/cercor/bhq058>.
- Jenkinson, M., Bannister, P., Brady, M., & Smith, S. (2002). Improved optimization for the robust and accurate linear registration and motion correction of brain images. *Neuroimage*, 17(2), 825–841.
- Kasai, K., Shenton, M. E., Salisbury, D. F., Onitsuka, T., Toner, S. K., Yurgelun-Todd, D., Kikinis, R., Jolesz, F. A., & McCarley, R. W. (2003). Differences and similarities in insular and temporal pole MRI gray matter volume abnormalities in first-episode schizophrenia and affective psychosis. *Archives of General Psychiatry*, 60(11), 1069–1077. <https://doi.org/10.1001/archpsyc.60.11.1069>.
- Kay, S. R., Fiszbein, A., & Opler, L. A. (1987). The positive and negative syndrome scale (PANSS) for schizophrenia. *Schizophrenia Bulletin*, 13(2), 261–276.
- Langer, N., Pedroni, A., Gianotti, L. R., Hänggi, J., Knoch, D., & Jäncke, L. (2012). Functional brain network efficiency predicts intelligence. *Human Brain Mapping*, 33(6), 1393–1406.
- Latora, V., & Marchiori, M. (2001). Efficient behavior of small-world networks. *Physical Review Letters*, 87(19), 198701. <https://doi.org/10.1103/PhysRevLett.87.198701>.
- Liu, H., Liu, Z., Liang, M., Hao, Y., Tan, L., Kuang, F., Yi, Y., Xu, L., & Jiang, T. (2006). Decreased regional homogeneity in schizophrenia: A resting state functional magnetic resonance imaging study. *Neuroreport*, 17(1), 19–22.
- Liu, Y., Liang, M., Zhou, Y., He, Y., Hao, Y., Song, M., Yu, C., Liu, H., Liu, Z., & Jiang, T. (2008). Disrupted small-world networks in schizophrenia. *Brain*, 131(Pt 4), 945–961. <https://doi.org/10.1093/brain/awn018>.
- Lynall, M. E., Bassett, D. S., Kerwin, R., McKenna, P. J., Kitzbichler, M., Muller, U., & Bullmore, E. (2010). Functional connectivity and brain networks in schizophrenia. *The Journal of Neuroscience*, 30(28), 9477–9487. <https://doi.org/10.1523/JNEUROSCI.0333-10.2010>.
- Maslov, S., & Sneppen, K. (2002). Specificity and stability in topology of protein networks. *Science*, 296(5569), 910–913. <https://doi.org/10.1126/science.1065103>.
- Mesholam-Gately, R. I., Giuliano, A. J., Goff, K. P., Faraone, S. V., & Seidman, L. J. (2009). Neurocognition in first-episode schizophrenia: A meta-analytic review. *Neuropsychology*, 23(3), 315–336. <https://doi.org/10.1037/a0014708>.
- Mesulam, M. M. (1998). From sensation to cognition. *Brain*, 121(Pt 6), 1013–1052.
- Navari, S., & Dazzan, P. (2009). Do antipsychotic drugs affect brain structure? A systematic and critical review of MRI findings. *Psychological Medicine*, 39(11), 1763–1777. <https://doi.org/10.1017/S0033291709005315>.
- Olson, I. R., Plotzker, A., & Ezzyat, Y. (2007). The enigmatic temporal pole: A review of findings on social and emotional processing. *Brain*, 130(Pt 7), 1718–1731. <https://doi.org/10.1093/brain/awm052>.
- Pettersson-Yeo, W., Allen, P., Benetti, S., McGuire, P., & Mechelli, A. (2011). Dysconnectivity in schizophrenia: Where are we now? *Neuroscience and Biobehavioral Reviews*, 35(5), 1110–1124. <https://doi.org/10.1016/j.neubiorev.2010.11.004>.
- Power, J. D., Barnes, K. A., Snyder, A. Z., Schlaggar, B. L., & Petersen, S. E. (2012). Spurious but systematic correlations in functional connectivity MRI networks arise from subject motion. *Neuroimage*, 59(3), 2142–2154. <https://doi.org/10.1016/j.neuroimage.2011.10.018>.
- Razafimandimby, A., Maiza, O., Herve, P. Y., Lecardeur, L., Delamillieure, P., Brazo, P., et al. (2007). Stability of functional language lateralization over time in schizophrenia patients. *Schizophrenia Research*, 94(1–3), 197–206. <https://doi.org/10.1016/j.schres.2007.04.011>.
- Repovs, G., Csemansky, J. G., & Barch, D. M. (2011). Brain network connectivity in individuals with schizophrenia and their siblings. *Biological Psychiatry*, 69(10), 967–973. <https://doi.org/10.1016/j.biopsych.2010.11.009>.
- Ribolsi, M., Koch, G., Magni, V., Di Lorenzo, G., Rubino, I. A., Siracusano, A., & Centonze, D. (2009). Abnormal brain

- lateralization and connectivity in schizophrenia. *Reviews in the Neurosciences*, 20(1), 61–70.
- Rimol, L. M., Hartberg, C. B., Nesvag, R., Fennema-Notestine, C., Hagler Jr., D. J., Pung, C. J., et al. (2010). Cortical thickness and subcortical volumes in schizophrenia and bipolar disorder. *Biological Psychiatry*, 68(1), 41–50. <https://doi.org/10.1016/j.biopsych.2010.03.036>.
- Rubinov, M., & Bullmore, E. (2013). Schizophrenia and abnormal brain network hubs. *Dialogues in Clinical Neuroscience*, 15(3), 339–349.
- Rubinov, M., & Sporns, O. (2010). Complex network measures of brain connectivity: Uses and interpretations. *Neuroimage*, 52(3), 1059–1069. <https://doi.org/10.1016/j.neuroimage.2009.10.003>.
- Rubinov, M., Knock, S. A., Stam, C. J., Micheloyannis, S., Harris, A. W., Williams, L. M., & Breakspear, M. (2009). Small-world properties of nonlinear brain activity in schizophrenia. *Human Brain Mapping*, 30(2), 403–416. <https://doi.org/10.1002/hbm.20517>.
- Salvador, R., Sarro, S., Gomar, J. J., Ortiz-Gil, J., Vila, F., Capdevila, A., et al. (2010). Overall brain connectivity maps show cortico-subcortical abnormalities in schizophrenia. *Human Brain Mapping*, 31(12), 2003–2014. <https://doi.org/10.1002/hbm.20993>.
- Shapleske, J., Rossell, S. L., Chitnis, X. A., Suckling, J., Simmons, A., Bullmore, E. T., et al. (2002). A computational morphometric MRI study of schizophrenia: Effects of hallucinations. *Cerebral Cortex*, 12(12), 1331–1341.
- Shenton, M. E., Dickey, C. C., Frumin, M., & McCarley, R. W. (2001). A review of MRI findings in schizophrenia. *Schizophrenia Research*, 49(1–2), 1–52.
- Skudlarski, P., Jagannathan, K., Anderson, K., Stevens, M. C., Calhoun, V. D., Skudlarska, B. A., & Pearlson, G. (2010). Brain connectivity is not only lower but different in schizophrenia: A combined anatomical and functional approach. *Biological Psychiatry*, 68(1), 61–69. <https://doi.org/10.1016/j.biopsych.2010.03.035>.
- Smith, S. M., Miller, K. L., Salimi-Khorshidi, G., Webster, M., Beckmann, C. F., Nichols, T. E., Ramsey, J. D., & Woolrich, M. W. (2011). Network modelling methods for FMRI. *Neuroimage*, 54(2), 875–891. <https://doi.org/10.1016/j.neuroimage.2010.08.063>.
- Sommer, I., Ramsey, N., Kahn, R., Aleman, A., & Bouma, A. (2001). Handedness, language lateralisation and anatomical asymmetry in schizophrenia: Meta-analysis. *The British Journal of Psychiatry*, 178, 344–351.
- Sporns, O. (2011). The human connectome: A complex network. *Annals of the New York Academy of Sciences*, 1224, 109–125. <https://doi.org/10.1111/j.1749-6632.2010.05888.x>.
- Sporns, O., & Zwi, J. D. (2004). The small world of the cerebral cortex. *Neuroinformatics*, 2(2), 145–162. <https://doi.org/10.1385/NI:2:2:145>.
- Stephan, K. E., Friston, K. J., & Frith, C. D. (2009). Dysconnection in schizophrenia: From abnormal synaptic plasticity to failures of self-monitoring. *Schizophrenia Bulletin*, 35(3), 509–527. <https://doi.org/10.1093/schbul/sbn176>.
- Sun, Y., Yin, Q., Fang, R., Yan, X., Wang, Y., Bezerianos, A., Tang, H., Miao, F., & Sun, J. (2014). Disrupted functional brain connectivity and its association to structural connectivity in amnesic mild cognitive impairment and Alzheimer's disease. *PLoS One*, 9(5), e96505. <https://doi.org/10.1371/journal.pone.0096505>.
- Sun, Y., Chen, Y., Collinson, S. L., Bezerianos, A., & Sim, K. (2017a). Reduced hemispheric asymmetry of brain anatomical networks is linked to schizophrenia: A connectome study. *Cerebral Cortex*, 27(1), 602–615. <https://doi.org/10.1093/cercor/bhv255>.
- Sun, Y., Dai, Z., Li, J., Collinson, S. L., & Sim, K. (2017b). Modular-level alterations of structure-function coupling in schizophrenia connectome. *Human Brain Mapping*, 38(4), 2008–2025. <https://doi.org/10.1002/hbm.23501>.
- Sun, Y., Li, J., Suckling, J., & Feng, L. (2017c). Asymmetry of hemispheric network topology reveals dissociable processes between functional and structural brain connectome in community-living elders. *Frontiers in Aging Neuroscience*, 9, 361. <https://doi.org/10.3389/fnagi.2017.00361>.
- Thompson, S. A., Patterson, K., & Hodges, J. R. (2003). Left/right asymmetry of atrophy in semantic dementia: Behavioral-cognitive implications. *Neurology*, 61(9), 1196–1203.
- Tian, L., Wang, J., Yan, C., & He, Y. (2011). Hemisphere- and gender-related differences in small-world brain networks: A resting-state functional MRI study. *Neuroimage*, 54(1), 191–202. <https://doi.org/10.1016/j.neuroimage.2010.07.066>.
- Tzourio-Mazoyer, N., Landeau, B., Papathanassiou, D., Crivello, F., Etard, O., Delcroix, N., Mazoyer, B., & Joliot, M. (2002). Automated anatomical labeling of activations in SPM using a macroscopic anatomical parcellation of the MNI MRI single-subject brain. *Neuroimage*, 15(1), 273–289. <https://doi.org/10.1006/nimg.2001.0978>.
- van den Heuvel, M. P., & Fornito, A. (2014). Brain networks in schizophrenia. *Neuropsychology Review*, 24(1), 32–48. <https://doi.org/10.1007/s11065-014-9248-7>.
- van den Heuvel, M. P., Stam, C. J., Kahn, R. S., & Hulshoff Pol, H. E. (2009). Efficiency of functional brain networks and intellectual performance. *The Journal of Neuroscience*, 29(23), 7619–7624. <https://doi.org/10.1523/JNEUROSCI.1443-09.2009>.
- van den Heuvel, M. P., Sporns, O., Collin, G., Scheewe, T., Mandl, R. C., Cahn, W., et al. (2013). Abnormal rich club organization and functional brain dynamics in schizophrenia. *JAMA Psychiatry*, 70(8), 783–792. <https://doi.org/10.1001/jamapsychiatry.2013.1328>.
- Van Dijk, K. R., Sabuncu, M. R., & Buckner, R. L. (2012). The influence of head motion on intrinsic functional connectivity MRI. *Neuroimage*, 59(1), 431–438. <https://doi.org/10.1016/j.neuroimage.2011.07.044>.
- van Erp, T. G., Hibar, D. P., Rasmussen, J. M., Glahn, D. C., Pearlson, G. D., Andreassen, O. A., et al. (2016). Subcortical brain volume abnormalities in 2028 individuals with schizophrenia and 2540 healthy controls via the ENIGMA consortium. *Molecular Psychiatry*, 21(4), 585. <https://doi.org/10.1038/mp.2015.118>.
- Wang, L., Metz, P. D., Honer, W. G., & Woodward, T. S. (2010). Impaired efficiency of functional networks underlying episodic memory-for-context in schizophrenia. *The Journal of Neuroscience*, 30(39), 13171–13179. <https://doi.org/10.1523/JNEUROSCI.3514-10.2010>.
- Wang, Z., Dai, Z., Gong, G., Zhou, C., & He, Y. (2015). Understanding structural-functional relationships in the human brain: A large-scale network perspective. *Neuroscientist*, 21(3), 290–305. <https://doi.org/10.1177/1073858414537560>.
- Wang, X., Zhang, Y., Long, Z., Zheng, J., Zhang, Y., Han, S., et al. (2017). Frequency-specific alteration of functional connectivity density in antipsychotic-naïve adolescents with early-onset schizophrenia. *Journal of Psychiatric Research*, 95, 68–75.
- Watts, D. J., & Strogatz, S. H. (1998). Collective dynamics of 'small-world' networks. *Nature*, 393(6684), 440–442. <https://doi.org/10.1038/30918>.
- Wu, K., Taki, Y., Sato, K., Kinomura, S., Goto, R., Okada, K., Kawashima, R., He, Y., Evans, A. C., & Fukuda, H. (2012). Age-related changes in topological organization of structural brain networks in healthy individuals. *Human Brain Mapping*, 33(3), 552–568. <https://doi.org/10.1002/hbm.21232>.
- Xia, M., Wang, J., & He, Y. (2013). BrainNet viewer: A network visualization tool for human brain connectomics. *PLoS One*, 8(7), e68910. <https://doi.org/10.1371/journal.pone.0068910>.

- Yan, C. G., & Zang, Y. F. (2010). DPARSF: A MATLAB toolbox for "pipeline" data analysis of resting-state fMRI. *Frontiers in Systems Neuroscience*, 4, 13. <https://doi.org/10.3389/fnsys.2010.00013>.
- Yan, C. G., Craddock, R. C., Zuo, X. N., Zang, Y. F., & Milham, M. P. (2013). Standardizing the intrinsic brain: Towards robust measurement of inter-individual variation in 1000 functional connectomes. *Neuroimage*, 80, 246–262. <https://doi.org/10.1016/j.neuroimage.2013.04.081>.
- Yu, Q., Plis, S. M., Erhardt, E. B., Allen, E. A., Sui, J., Kiehl, K. A., Pearlson, G., & Calhoun, V. D. (2011). Modular organization of functional network connectivity in healthy controls and patients with schizophrenia during the resting state. *Frontiers in Systems Neuroscience*, 5, 103. <https://doi.org/10.3389/fnsys.2011.00103>.
- Yu, Q., Sui, J., Liu, J., Plis, S. M., Kiehl, K. A., Pearlson, G., & Calhoun, V. D. (2013). Disrupted correlation between low frequency power and connectivity strength of resting state brain networks in schizophrenia. *Schizophrenia Research*, 143(1), 165–171. <https://doi.org/10.1016/j.schres.2012.11.001>.
- Yu, R., Chien, Y. L., Wang, H. L. S., Liu, C. M., Liu, C. C., Hwang, T. J., Hsieh, M. H., Hwu, H. G., & Tseng, W. Y. I. (2014). Frequency-specific alternations in the amplitude of low-frequency fluctuations in schizophrenia. *Human Brain Mapping*, 35(2), 627–637.
- Zalesky, A., Fornito, A., & Bullmore, E. (2012). On the use of correlation as a measure of network connectivity. *Neuroimage*, 60(4), 2096–2106. <https://doi.org/10.1016/j.neuroimage.2012.02.001>.